International Journal of Pharmaceutics 389 (2010) 232–243

Contents lists available at ScienceDirect

International Journal of Pharmaceutics

journal homepage: www.elsevier.com/locate/ijpharm

Pharmaceutical Nanotechnology

Lipid-mediated delivery of RNA is more efficient than delivery of DNA in non-dividing cells

S. Zou[a], K. Scarfo[a], M.H. Nantz[b], J.G. Hecker[a,*]

[a] Department of Anesthesiology and Critical Care, University of Pennsylvania School of Medicine, Morgan 305, 3620 Hamilton Walk, Philadelphia, PA 19104-6112, United States
[b] Department of Chemistry, University of Louisville, Louisville, KY 40292, United States

ARTICLE INFO

Article history:
Received 10 November 2009
Received in revised form 4 January 2010
Accepted 10 January 2010
Available online 18 January 2010

Keywords:
Non-viral
Lipid-mediated
Gene delivery
Transfection
RNA
DNA
siRNA
Primary neurons
Post-mitotic

ABSTRACT

The design of appropriate gene delivery systems is essential for the successful application of gene therapy to clinical medicine. Cationic lipid-mediated delivery is a viable alternative to viral vector-mediated gene delivery in applications where transient gene expression is desirable. However, cationic lipid-mediated delivery of DNA to post-mitotic cells such as neurons is often reported to be of low efficiency, due to the presumed inability of the DNA to translocate to the nucleus. Lipid-mediated delivery of RNA is an attractive alternative to non-viral DNA delivery in some clinical applications, because transit across the nuclear membrane is not necessary. Here we report a comparative investigation of cationic lipid-mediated delivery of RNA versus DNA vectors encoding the reporter gene green fluorescent protein (GFP) in Chinese Hamster Ovary (CHO) and NIH3T3 cells following chemical inhibition of proliferation, and in primary mixed neuronal cell cultures. Using optimized formulations and transfection procedures, we assess gene expression by flow cytometry to specifically address some of the advantages and disadvantages of lipid-mediated RNA and DNA gene transfer. Despite inhibition of cell proliferation, over 45% of CHO cells express GFP after lipid-mediated transfection with RNA vectors. Transfection efficiency of DNA encoding GFP in proliferation-inhibited CHO cells was less than 5%. Detectable expression after RNA transfection occurs at least 3 h earlier than after DNA transfection, but DNA transfection eventually produces a mean level of per cell GFP expression (as assayed by flow cytometry) that is higher than after RNA transfection. Transfection of proliferation-inhibited NIH3T3 cells and primary mixed neuronal cultures produced similar results, with RNA encoded GFP expression in 2–4 times the number of cells as after DNA encoded GFP expression. These results demonstrate the increased efficiency of RNA transfection relative to DNA transfection in non-dividing cells. We used firefly luciferase encoded by RNA and DNA vectors to investigate the time course of gene expression after delivery of RNA or DNA to primary neuronal cortical cells. Delivery of mRNA resulted in rapid onset (within 1 h) of luciferase expression after transfection, a peak in expression 5–7 h after transfection, and a return to baseline within 12 h after transfection. After DNA delivery significant luciferase activity did not appear until 7 h after transfection, but peak luciferase expression was always at least one order of magnitude higher than after RNA delivery. The peak expression after luciferase-expressing DNA delivery occurred 36–48 h after transfection and remained at a significant level for at least one week before dropping to baseline. This observation is consistent with our *in vivo* delivery results, which are shown as well. RNA delivery may therefore be more suitable for short-term transient gene expression due to rapid onset, shorter duration of expression and greater efficiency, particularly in non-dividing cells. Higher mean levels of expression per cell obtained following DNA delivery and the longer duration of expression confirm a continuing role for DNA gene delivery in clinical applications that require longer term transient gene expression.

1. Introduction

Gene therapy has the potential to significantly advance clinical medicine, although this potential is largely still unrealized. Long-term expression after gene therapy is useful for diseases which require chronic levels of protein expression, such as inherited enzyme deficiencies, or cancer, and for these diseases viral vectors may offer advantages. However, the risks and duration of gene delivery must also be closely matched to the proposed clinical application (Flotte, 2007). For some clinical applications only short-term gene expression is required or warranted. Pre-operative expression of neuroprotective gene sequences in the Central Nervous System (CNS), as well as attenuation of cell death following CNS trauma or stroke, are important potential clinical applications

* Corresponding author. Tel.: +1 215 349 5343; fax: +1 215 349 5078.
E-mail address: heckerj@uphs.upenn.edu (J.G. Hecker).

0378-5173/$ – see front matter © 2010 Elsevier B.V. All rights reserved.
doi:10.1016/j.ijpharm.2010.01.019

for transient gene expression. Clinical trials which use cationic lipids for delivery have mainly involved applications requiring brief expression of transgenes, such as therapies aimed at direct or immunological killing of tumor cells. The recent discovery of the critical roles that the small RNAs (siRNA, shRNA, microRNA) play in transcription and expression is an entirely new arena for short-term non-viral nucleic acids delivery.

Cationic lipid-mediated gene transfer is particularly suited for transient gene expression, both in basic research and in selected clinical applications. The delivery of nucleic acids by means of a non-viral cationic lipid may provide a more favorable risk/benefit analysis than viral vectors. Cationic lipid-mediated transfection also has other advantages over viral vectors, most notably safety, low immunogenicity, ease of preparation, and the ability to transfect vectors of nearly unlimited size (Li and Huang, 2006; Gao et al., 2007). Cationic lipids are commonly comprised of a polar headgroup and non-polar symmetric or dissymmetric carbon based tail. Appropriately structured cationic lipids condense and protect nucleic acids from degradation in the extracellular environment (Luo and Saltzman, 2000). Negatively charged nucleic acids condense and self-assemble into heterogeneous complexes of lipids and nucleic acids when mixed with cationic lipids (Felgner et al., 1995). The structure and size of these complexes affect transfection efficacy and vary with temperature, concentration, charge ratio, buffer, time, and lipid composition. Numerous laboratories (Felgner et al., 1987; Byk and Scherman, 2000), including our own (Niedzinski et al., 2002), have investigated the limiting parameters of cationic lipid-mediated transfection with the goal of improving transfection efficiency. While cationic lipid-mediated transfections work well with many types of cells (Felgner et al., 1987; Li and Huang, 2006; Gao et al., 2007), the transfection of primary cell lines remains a problem (Wangerek et al., 2001). There are four general barriers to lipid-mediated DNA transfection: (1) transport of the nucleic acid/lipid complex in the extracellular environment; (2) association and uptake of the nucleic acid/lipid complex by the target cell (Bally et al., 1999); (3) intracellular DNA release from the nucleic acid/lipid complex (Girao da Cruz et al., 2001); and (4) translocation of DNA to the nucleus (Mortimer et al., 1999). The primary barrier to DNA transfections in post-mitotic cells is assumed to be DNA translocation to the nucleus (Zabner et al., 1995).

Although adenovirus (Ad), some adeno-associated virus (AAV) serotypes (Taymans et al., 2007), or Herpes Simplex Virus (HSV) are effective in the CNS (Krisky et al., 1998), viral vectors have a long lag time before significant expression, in addition to the drawbacks previously discussed. Neuronal cells are regarded as difficult to transfect with non-viral techniques though, and this transfection difficulty is generally attributed to markedly reduced or absent mitotic activity in the post-mitotic neuronal cells (Wangerek et al., 2001). In proliferating cells, nuclear translocation is mainly passive, occurring during mitosis as the nuclear membrane breaks-down (Nicolau and Sene, 1982; Wilke et al., 1996; Bally et al., 1999). Some nuclear translocation does still occur in non-proliferating cells, which is probably the result of passive movement through the nuclear pore complex (NPC) (Wilson et al., 1995; Mattaj and Englmeier, 1998). To improve the efficiency of lipid-mediated DNA transfer some investigators have used nuclear localization sequences (NLS) (Aronsohn and Hughes, 1998; Melchior and Gerace, 1998) to target the NPC and thus to facilitate DNA entry into the nucleus.

As others have suggested, we propose that using RNA instead of DNA eliminates the necessity for nuclear translocation and thus has the potential to greatly improve transfection of post-mitotic cells. Lipid-mediated RNA and DNA delivery to proliferating cells (Malone et al., 1989) as well as intramuscular injection of naked RNA and DNA have been previously described (Wolff et al., 1990). In this study, the first to make a comparative analysis of cationic lipid-mediated RNA versus DNA gene delivery in proliferation-inhibited cells and primary mixed neuronal cultures, we explicitly test the hypothesis that RNA vector delivery is more efficient than DNA vector delivery. Our studies show that RNA is 2–5 times more efficient based on the percentage of cells transfected, as measured by flow cytometry.

2. Materials and methods

As a brief overview of our experiments, we first conducted repeated luciferase mRNA and DNA transfections in NIH3T3 and CHO cells, analyzing luciferase expression at multiple time points to determine the time of peak luciferase expression *in vitro*. We then repeated these experiments by transfecting CHO and NIH3T3 cells using GFP mRNA and DNA vectors so that transfections could be quantitatively analyzed for transfection efficacy, percentage of cells transfected, intensity, and toxicity using flow cytometry. We proliferation-inhibited dividing cells, transfected primary neuronal cells, and finally used these same methods to deliver and express in the CNS of the rat.

2.1. Non-neuronal cell maintenance

CHO cells (ATCC, Rockville, MD) were cultured in 75 cm^2 cell culture flasks with HAMS F12 media (Life Technologies, Gaithersburg, MD) containing 10% bovine calf serum at 37 °C in a 5% CO_2 environment. NIH3T3 cells (ATCC) are cultured in 75 cm^2 cell culture flasks with DMEM media (Life Technologies) containing 10% bovine calf serum at 37 °C in a 5% CO_2 environment. Both CHO and NIH3T3 cells were split 48 h prior to transfection and plated at 60% confluence.

2.2. Primary cell isolation and cultures

Primary neuronal cells were dissected from the cortex of day 17 Sprague–Dawley rat fetuses as previously described (McKinney et al., 1996). Briefly, fetal rat brains were removed and placed in ice cold sterile PBS where cortex was dissected and cleared of meninges. Cortical sections were transferred to a 60 mm Petri dish containing 4 ml PBS and minced into pieces of approximately 1 mm^3 in size, then transferred into a 15 ml sterile tube, supplemented with 4 ml neural basal medium containing 0.5 mM L-glutamine, 1× B27, and 50 ng/ml neural growth factor, supplemented with 0.25% trypsin–EDTA and 20 μl DNase I, and shaken for 30 min at 37 °C. The resultant suspension was mechanically forced through the small orifice of a Pasteur pipette tube to eliminate residual clumps of brain tissue, and then filtered through 40 μm nylon net to obtain single cell suspensions. Cells were spun down and resuspended in neural basal medium as above. 1×10^6 cells per ml were seeded onto poly-L-lysine pre-coated 24-well tissue culture dishes. Cells were cultured in a 5% CO_2 incubator at 37 °C, and maintained in culture for two weeks prior to transfection to allow the development of the correspondent mature phenotype of human cortical neurons. Every 3–4 days one half of the medium was replaced with medium containing fresh neural growth factor. Cultures of cortical neuron prepared in this fashion usually contained less than 10% glial cells (McKinney et al., 1996).

2.3. Inhibition of proliferation

We tested our hypothesis that proliferation was necessary for efficient transfection of non-viral DNA vectors, but not for mRNA vectors. In one half of the cell cultures we used roscovitine to inhibit cell proliferation, and compared the intensity and fraction of GFP-positive cells at the two time points of peak expression for mRNA and DNA in both CHO and NIH3T3 cells, respectively. CHO and

NIH3T3 cells were treated with 15 μM roscovitine (Sigma) diluted in serum free media 24 h prior to transfection. This concentration was determined after a series of experiments to examine cell viability. We reproducibly measured approximately 67% of the cells in G0G1, 33% in S-phase, and less than 1% in G2M after inhibition of proliferation (data not shown).

2.4. Nucleic acid delivery vectors

2.4.1. eGFP and luciferase DNA vectors

The blank pND expression vector (gift of Gary Rhodes, Ph.D., University of California, Davis) contains the human CMV immediate early promoter (HCMV IE1) and CMV IE1 intron, and a Multiple Cloning Site (MCS), followed by the RNA terminator/polyadenylation site derived from bovine growth hormone (BGH) in a pUC19 replicon (Chapman et al., 1991). eGFP and luciferase coding sequences were inserted into the multiple cloning site to form the eGFP DNA Vector (pND.eGFP) and luciferase DNA vector (pND.Luc). DNA vectors for GFP and luciferase were identical except for coding sequence of the reporter.

2.4.2. eGFP and luciferase mRNA transcripts

We constructed and compared three different mRNA vectors and found similar results for each. Plasmid pT7Omega.lucA50 (gift from Robert Malone, Ph.D., University of California, Davis) was used for initial experiments to optimize conditions for lipoplex formulation and delivery. The β-globin luciferase plasmid, which contains β-globin stabilizing elements, was also used for time course experiments in primary neuronal cells (gift of Jon Wolf, M.D., University of Wisconsin). Plasmid pTEVA50 (gift from K. Kariko, Ph.D., University of Pennsylvania) was also used for proliferation inhibition experiments in CHO and NIH3T3 cells as well as in primary neuronal cell cultures.

pT7OmegaA50 (Gallie vector) contains a T7 promoter driven encoding sequence stabilized by the Omega 5′ untranslated transcriptional enhancer region (UTR) and 3′ poly-adenylated tail from Tobacco Mosaic Virus (TMV) (Gallie and Walbot, 1990; Wells et al., 1998). 5′ and 3′ Untranslated Regions (UTRs) have been shown to improve intracellular mRNA stability and lead to translational enhancements in eukaryotic as well as prokaryotic cells (Gallie and Walbot, 1990; Wells et al., 1998). Luciferase and eGFP sequences were subcloned into the Gallie TMV vectors. β-globin enhanced Green Fluorescent Protein (eGFP) vector was formed by subcloning eGFP into the β-globin vector using Nco1 and Xba1 restriction enzymes. β-globin eGFP and Gallie TMV vectors were linearized with restriction enzyme Dra I after elimination of RNases by proteinase K treatment and phenol/chloroform extraction. TEV vectors were linearized with Nde1 after similar treatment. After precipitation in ethanol, linearized DNA templates were transcribed *in vitro* using the T7 mMessage mMachine transcription kit (Ambion, Austin, TX). As described in the Results Section, all three RNA vectors gave very similar time courses and levels of expression.

2.4.3. Formulation of DNA or RNA with lipid to form lipoplexes

MLRI and similar cationic lipids were described previously by Balasubramaniam et al. (1996), Bennett et al. (1995, 1996) and Felgner et al. (1994). Briefly, MLRI was prepared by adding chloroform to dry MLRI (dissymmetric Myristoyl (14:0) and Lauroyl (12:1) Rosenthal Inhibitor-substituted compound formed from the tetraalkylammonium glycerol-based DORI) and mixed 50:50 with L-dioleoyl phosphatidyl-ethanolamine (DOPE) in chloroform. The TransFast™ Transfection Reagent is comprised of the synthetic cationic lipid (+)-N,N{bis (2-hydroxyehyl)}-N-methyl-N-{2,3-di(tetradecanolyloxy)propyl} ammonium iodide and the neutral lipid, DOPE (Promega, WI). Liposome reagents specifically designed for transfection applications often incorporate synthetic cationic lipids, such as the neutral lipid DOPE or cholesterol, to improve efficacy. DOPE has been demonstrated to enhance the gene transfer ability of certain cationic lipids (Felgner et al., 1994). Following the manufacturer's instructions Transfast was rehydrated in water and stored overnight. After individual optimization and simultaneous comparison of several commercially available cationic lipids, the lipids MLRI and TransFast™ Transfection Reagent (Promega, Madison, WI) were chosen for their efficiency and low cytotoxicity.

2.4.4. Lipid formulation for cell transfection

Times for maximal luciferase expression were determined first in luciferase vector lipoplex transfections by varying charge ratio, dose, formulation time, concentration, and temperature (Fujii et al., 2002). These results were then compared and confirmed using GFP vectors by flow cytometry (below) to determine the maximum percentage of cells expressing GFP, which could be different than the time of maximal luciferase expression in cell lysates. Transfection formulations of GFP encoding RNA and DNA vectors were optimized using flow cytometry to obtain the maximum percentage of GFP expressing cells. Optimized GFP-encoding mRNA and DNA vectors were delivered to CHO cells and were analyzed at times that overlapped the times of the peaks found after luciferase transfection using FASCcan or Caliper flow cytometry (Becton Dickinson) and Cell Quest software (Becton Dickinson) to determine the peak of fractional expression. We then repeated these experiments at the peak fractional expression for the GFP-expressing RNA and DNA vector lipoplexes, 7 and 24 h respectively. Cells were transfected with 1 μg of either DNA or mRNA. Although 1 μg each of DNA and RNA are not equal numbers of nucleic acid copies, lipid nucleic acid complexes are formulated based on an equal lipid to nucleic acid charge ratio. The lipid/nucleic acid complex (lipoplex) is formed by the addition of 1 μg of nucleic acid (mRNA or DNA) to serum free media, vortexing, and then adding lipid to produce a 3:1 charge ratio. For *in vitro* experiments plasmid DNA and MLRI were added to OptiMem solution. The final solution, in 200 μl, is vortexed and incubated for 1 h at room temperature (RT) prior to aspiration of growth media from the cells and application of transfection formulation to the cells. After 1 h of incubation the cells are supplemented with 1 ml of growth media. Cells were harvested for flow cytometry analysis 24 h after GFP DNA vector lipoplex transfections and 7 h after RNA transfections.

2.4.5. Lipid formulation for in vivo transfection

Mixtures for *in vivo* experiments contained only DNA solution and lipid, without OptiMem, in order to minimize injected volume. Mixtures were incubated at 37 °C for 45–60 min prior to transfection *in vitro* and for 30 min prior to delivery *in vivo*. *In vivo* delivery to the rat CSF required approximately 15 min after the needle localization into the lateral ventricle or cisterna magna, resulting in a total effective incubation time of 45–60 min.

2.4.6. Flow cytometry analysis

mRNA and DNA GFP transfections in CHO and NIH3T3 cells were compared at the time corresponding to the time of maximal fraction of cells expressing GFP. We compared the intensity and fraction of GFP-positive primary neuronal cells, which are non-proliferative, after transfection with the same GFP mRNA and DNA vectors. Due to the difficulty of isolating and preparing primary neuronal cells, and of flow analysis of neurons, only a limited number of flow cytometry measurements were made with neuronal cells.

CHO, NIH3T3 and primary neuronal cells were trypsinized and washed twice in Dulbecco's phosphate buffered saline with Ca^{2+} (DPBS) and re-suspended in DPBS. Cells were harvested and ana-

lyzed at the time point corresponding to the maximum percentage of cells expressing GFP, 7 h for mRNA transfection and 24 h for DNA transfections. GFP fluorescence was measured using a dual channel FACScan or multi-channel Caliber flow cytometer (Becton Dickinson, San Jose, CA) equipped with a single 488 nm argon laser. GFP fluorescence was measured with a 530 nm band pass filter. Data was analyzed with CellQuest software (Becton Dickinson). 10,000 events were collected per sample. All experiments were conducted at least three times for CHO and NIH3T3 cells, and twice for primary neuronal cells.

2.4.7. Cell toxicity analysis

CHO and NIH3T3 cells were trypsinized and washed twice in Dulbecco's phosphate buffered saline with Ca^{2+} (DPBS), re-suspended, and incubated for 30 min in annexin V conjugated with biotin (CalTag, Burlingame, CA) in DPBS. After a DPBS wash, the cells were re-suspended for 30 min in streptavidin conjugated with a Tri-Color fluorophore (CalTag, Burlingame, CA) in DPBS. The cells were analyzed using a dual channel FACScan as described above. Tri-Color fluorescence was measured with a 675 band pass filter.

2.4.8. Time course of luciferase expression in primary neurons after mRNA versus DNA transfection

We first obtained *in vitro* time course measurements in NIH3T3 and CHO cells (results not shown) to plan for transfections of the non-proliferating neuronal cells. At various time points after transfection of primary cortical neurons, cells were lysed in 200 μl of lysis buffer. 20 μl of lysate was analyzed by luciferase assay using an Enhanced Luciferase assay Kit (BD Bioscience). Quantitative luminescence was measured using a Monolight 2010 (Analytical Luminescence Laboratory, now Becton Dickinson).

2.4.9. In vivo luciferase-expressing mRNA vector delivery to rat brain

Finally we repeated and confirmed the time course of expression in primary neuronal cell cultures using our mRNA and DNA luciferase vectors. As an example of *in vivo* luciferase expression we show results in rat brain 7 h after RNA delivery to the lateral ventricle Fig. 8. To demonstrate the widespread distribution, uptake and expression that is possible after non-viral, cationic lipid-mediated gene delivery of mRNA vectors, we infused an optimized formulation of luciferase-encoding mRNA transcript into the lateral ventricle of rat brain. Direct injections were performed using standard techniques that we previously reported (Hecker et al., 2001; Anderson et al., 2003). Under an approved animal care protocol, adequately anesthetized animal subjects (250–300 g Sprague–Dawley rats) were mounted in the stereotaxic small animal surgery frame (Stoelting, Wood Dale, IL). Using sterile techniques, previously optimized formulations were delivered using coordinates of 0.9–1.0 mm posterior and 1.5 mm lateral of midline relative to bregma, at a depth of approximately 3–3.5 mm. After aspiration of CSF to verify intraventricular canula placement, the transfection formulation was infused over 40 min using a syringe infusion pump (Model 101, Stoelting). Animals were closely monitored for signs of discomfort, toxicity, or neurologic injury, and none were observed.

2.4.10. Tissue preparation for reporter protein localization after mRNA delivery

Seven hours after mRNA vector delivery, the animal subjects were deeply anesthetized and perfused through the ascending aorta with saline, followed by 4% paraformaldehyde in 0.1 M, pH 7.4, sodium phosphate-buffered saline (PBS). The brain was removed, dissected, post-fixed in paraformaldehyde fixative overnight at 4 °C, and was then placed in PBS containing 20% glycerol at 4 °C. After blocking, brains were cryosectioned in the coronal plane following standard techniques, beginning approxi-

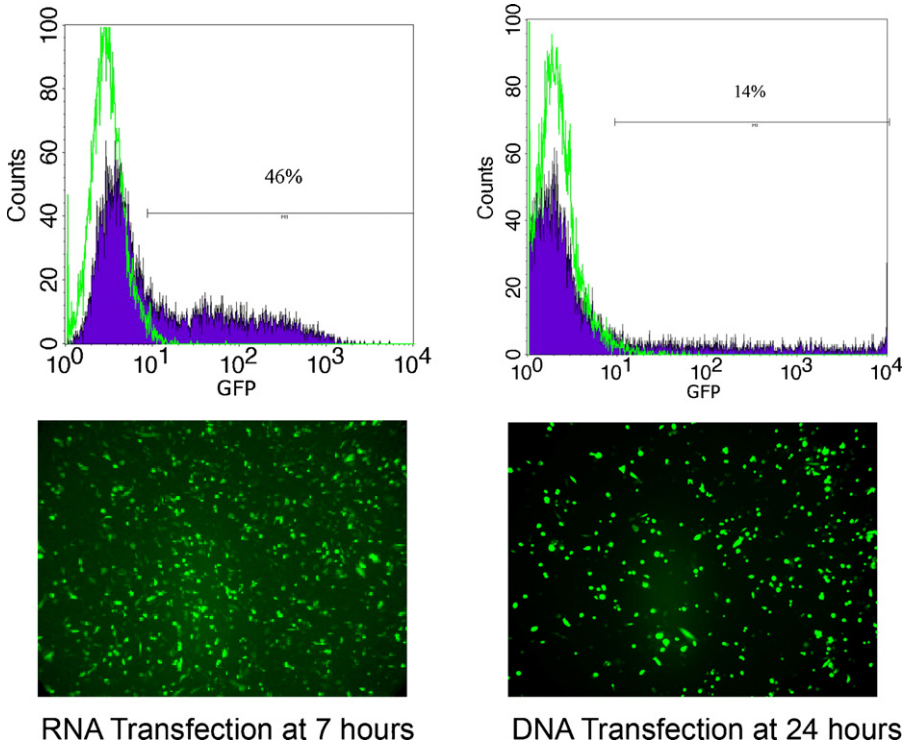

Fig. 1. FACScan analysis of cationic lipid-mediated RNA and DNA GFP transfection in CHO cells. This figure is an example of the fraction of CHO cells transfected by RNA versus DNA in the absence of any inhibition of proliferation. Top panels show representative flow cytometry for RNA (left) versus DNA (right) transfections.

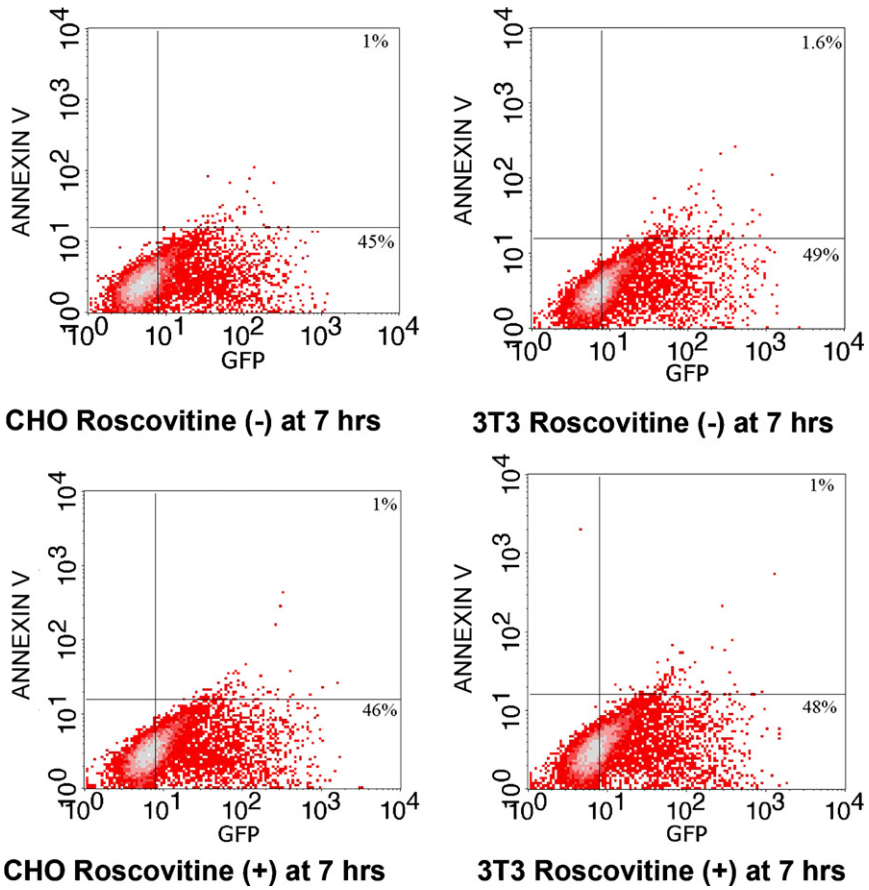

Fig. 2. FACScan analysis of cationic lipid-mediated RNA GFP transfection of proliferation-inhibited CHO and NIH3T3 cells. Results are presented at the time point at which the maximum percentage of cells expresses GFP. Representative results show the percentage of GFP-expressing cells after RNA transfection at 7 h in roscovitine treated (+) and untreated (−) CHO and NIH3T3 cells. In this figure, RNA transfections, the two panels of flow cytometry results on the left hand side are CHO cells, while the right two panels are NIH3T3 cells. The CHO and NIH3T3 cells in the bottom two panels were treated with roscovitine to inhibit proliferation, while the top two panels show CHO and NIH3T3 cells in the absence of roscovitine. Each flow cytometry result shows Annexin V to detect early apoptosis on the vertical axis versus GFP on the horizontal axis. Fig. 3 shows similar results for DNA GFP transfections in an identical presentation. Inhibition of proliferation has no effect on transfection with RNA on either cell type, but dramatically reduces the fraction of cells transfected with DNA vectors in both cell types in Fig. 3.

mately 6–7 mm anterior relative to bregma. Ten series of 30-μm serial sections were collected for each brain.

2.4.11. Diaminobenzidine immunohistochemistry

Diaminobenzidine (DAB) and secondary fluorescent immunohistochemistry protocols were optimized previously for expression using multiple DNA and mRNA vectors (Hecker et al., 2001; Anderson et al., 2003). Negative controls for these optimizations included no primary antibody and no secondary antibody controls on slide-mounted sections or in 24-well plates. To ensure identical, simultaneous processing free-floating sections in 24-well plates were stained using the ExtrAvidin® peroxidase system (Sigma, St. Louis, MO). For comparison, experiments were also processed using sections mounted on poly-L-lysine-coated microscope slides (Columbia Diagnostics, Inc., Springfield, VA) and air-dried for a minimum of 2 h. H_2O_2 (0.1% H_2O_2 for 15 min) was used to eliminate staining caused by endogenous peroxidase activity. Sections were fixed in 4% paraformaldehyde and pre-treated with pretreated with H_2O_2 before washing in modified PBS. Sections were incubated in blocking buffer (0.3% Triton X-100, 3% bovine serum albumin (BSA), 10% normal goat serum (NGS), Ca^{+2} and Mg^{+2}-free PBS) for 2 h at room temperature. Primary antibodies were appropriately diluted in blocking buffer and sections were incubated at 4 °C overnight. Sections were then washed and incubated with the biotin-conjugated secondary antibody, which targets the primary antibody host species, for 1 h at room temperature. Sections were again washed and incubated with the tertiary horseradish peroxidase-conjugated probe for 1 h at room temperature, washed again, and incubated in 50 mM Tris–HCl at pH 7.6 for 5 min at room temperature. For detection of target proteins sections are incubated with 0.5 mg/ml DAB with 0.03% H_2O_2 as the peroxidase substrate. Following the optimization described above, the following antibodies and dilutions were found to be optimal. Primary antibodies: mouse monoclonal neuron specific nuclear protein anti-NeuN (MAB377, 1:50; Chemicon, Temecula, CA); rabbit polyclonal antiluciferase antibody (CR2029R, 1:50; Cortex Biochem, San Leandro, CA). The NeuN antibody was used for comparisons of the number of neurons that can be identified in each section (data not shown). We used a Nikon 600 microscope with camera mount for photographic documentation of results. Film negatives or slides were scanned into Photoshop 5.0 using a Photoshop plug-in and Polaroid SprintScan slide scanner at a resolution of 2700 dpi. Photographs were printed using Photoshop 5.0 (Adobe, Seattle, WA) on a Fuji Pictrography 3000 (Fuji Photo Film, Elmsford, NY) at 320 dpi. Later experiments were documented on a Nikon Eclipse TS100 Inverted microscope (Japan) with a high resolution digital camera (SPOT, Diagnostic Instruments).

3. Results

Niedzinski et al. (2002) and Fujii et al. (2002) investigated previously the limiting parameters of cationic lipid-mediated

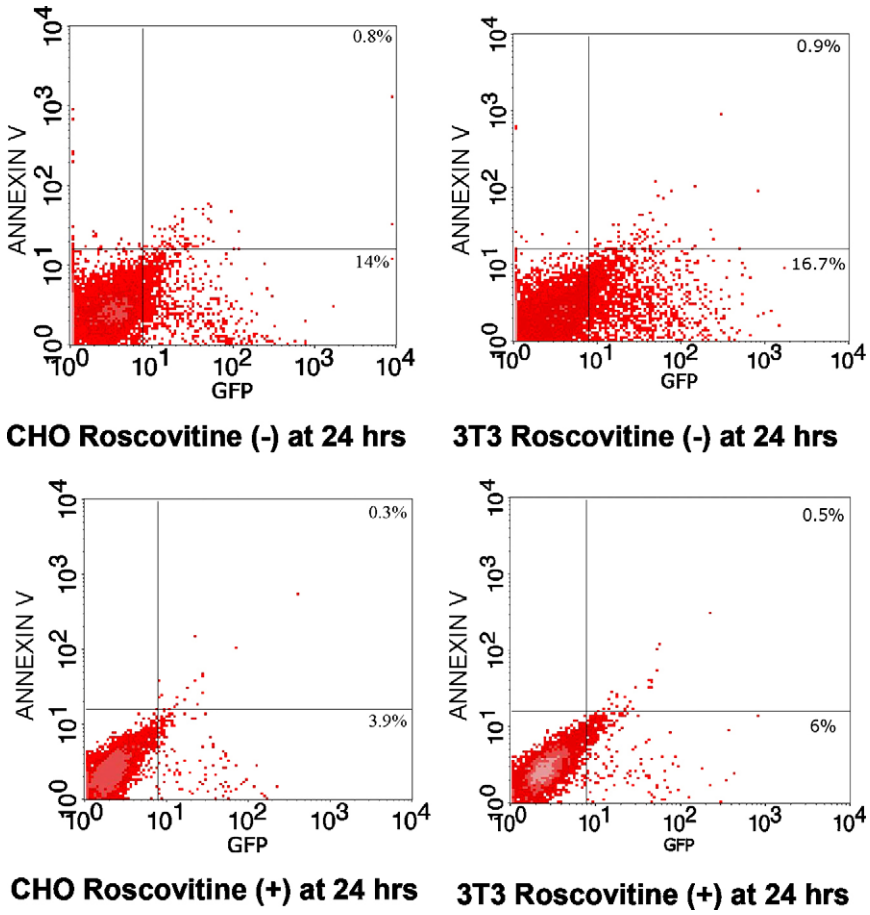

Fig. 3. FACScan analysis of cationic lipid-mediated DNA GFP transfection of proliferation-inhibited CHO and NIH3T3 cells. Representative results show the percentage of GFP-expressing CHO cells after DNA transfection 24 h in roscovitine treated (+) and untreated (−) CHO and NIH3T3 cells.

transfection with the goal of improving transfection efficiency. For RNA vectors we found 6–7 h to be the peak using either luciferase cell lysis analysis or GFP flow cytometry results. For DNA vectors we found that the GFP peak in expression (24–36 h) as a percentage of cells expressing GFP occurred slightly earlier than the peak in luciferase expression and protein accumulation (36–48 h). We chose to compare simultaneous RNA versus DNA transfections using flow cytometry at 7 and 24 h, respectively, based on the peaks we found in these time course experiments. We chose to analyze DNA transfections at 24 h for two reasons. One, based on a comparison of the time courses of expression of luciferase cell lysis analysis and GFP flow cytometry analysis for percentage of cells transfected, 24 h is sufficient for a robust transfection. Two, when we use roscovitine to inhibit cell proliferation, we found that the cells would begin to escape cell cycle arrest over time and return to asynchrony, and at 24 h we still have significant proliferation arrest.

3.1. GFP RNA compared to DNA vector delivery in CHO cells

Results are presented at the time point for the maximum percentage of cells expressing GFP. Fig. 1 is an example of the fraction of CHO cells transfected by RNA versus DNA in the absence of any inhibition of proliferation. As shown in Fig. 1 GFP RNA vectors transfected over 45% of CHO cells by 7 h, but only approximately 14% were transfected with the GFP DNA vector by 24 h. The mean level of expression per cell as measured by Cell Quest analysis of GFP intensity was greater than 5 times higher in DNA transfected cells relative to RNA transfected cells, despite the higher copy number of RNA transcripts delivered (1 μg each of mRNA or DNA, respectively). Examples of the fluorescent GFP-expressing cells are shown under each panel.

3.1.1. GFP RNA and DNA vector delivery in proliferation-inhibited CHO and NIH3T3 cells

Next, previously optimized GFP-encoding mRNA and DNA vectors were delivered to roscovitine proliferation-inhibited CHO and NIH3T3 cells and analyzed by flow cytometry. We reproducibly measured approximately 67% of the cells in G0G1, 33% in S-phase, and less than 1% in G2 M after inhibition of proliferation (data not shown). Results are again presented at the time point at which the maximum percentage of cells expresses GFP for each vector. As shown in Figs. 2 and 3, in simultaneous transfections GFP RNA vectors transfected approximately 50% of proliferation-inhibited cells, regardless of whether proliferation was inhibited or not. But only approximately 5% of proliferation-inhibited NIH3T3 cells were transfected with a GFP DNA vector. In Fig. 2, RNA transfections, the two panels of flow cytometry results on the left hand side are CHO cells, while the right two panels are NIH3T3 cells. The CHO and NIH3T3 cells in the bottom two panels were treated with roscovitine to inhibit proliferation, while the top two panels show CHO and NIH3T3 cells in the absence of roscovitine. Each flow cytometry result shows Annexin V to detect early apoptosis on the vertical axis versus GFP on the horizontal axis. Fig. 3 shows similar results for DNA GFP transfections in an identical presentation. As can be seen in Fig. 2, inhibition of proliferation has no effect on transfection with RNA on either cell type, but dramatically reduces the fraction of cells transfected with DNA vectors in both cell types in Fig. 3,

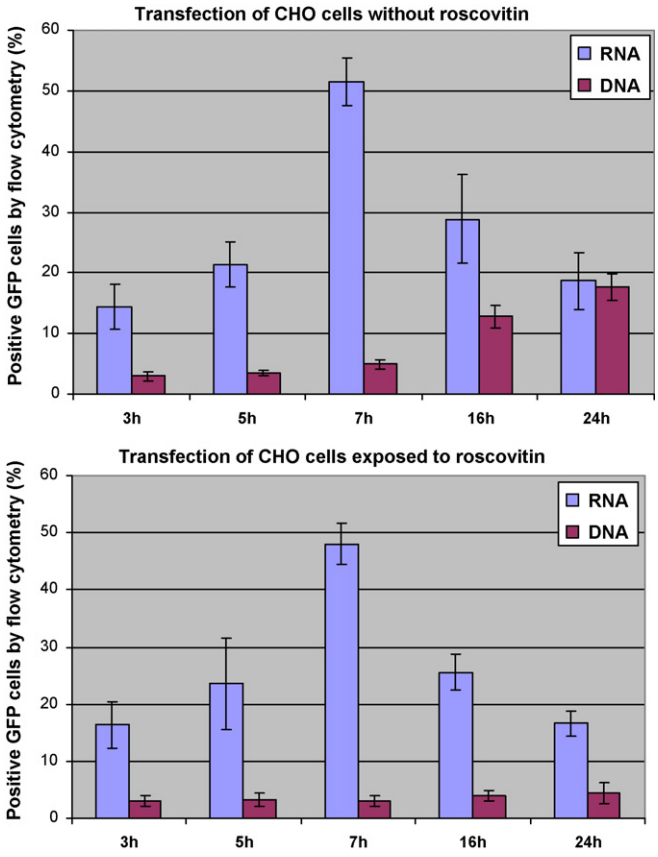

Fig. 4. Time course of GFP expression in CHO cells with and without proliferation-inhibition by roscovitine. This figure and Fig. 5 summarize the results of multiple transfections of GFP DNA versus RNA vectors over time. The percent of GFP positive cells by flow cytometry was plotted versus time in hours. This figure shows the peak in fraction of CHO cells expressing GFP after transfection, and the absence of any effect from application of roscovitine using RNA, in contrast to the effect of roscovitine with DNA transfection. Roscovitine has no effect on GFP RNA transfections, and the peak at 7 h using RNA vectors is clearly illustrated in this figure. DNA transfections, in contrast, reach only 18% in the absence of roscovitine, and less than 5% with proliferation-inhibition roscovitine (+). The fraction of cells which express GFP after GFP DNA transfection in the absence of treatment with roscovitine is still increasing after 24 h, but is blocked at low level by roscovitine in the bottom panel.

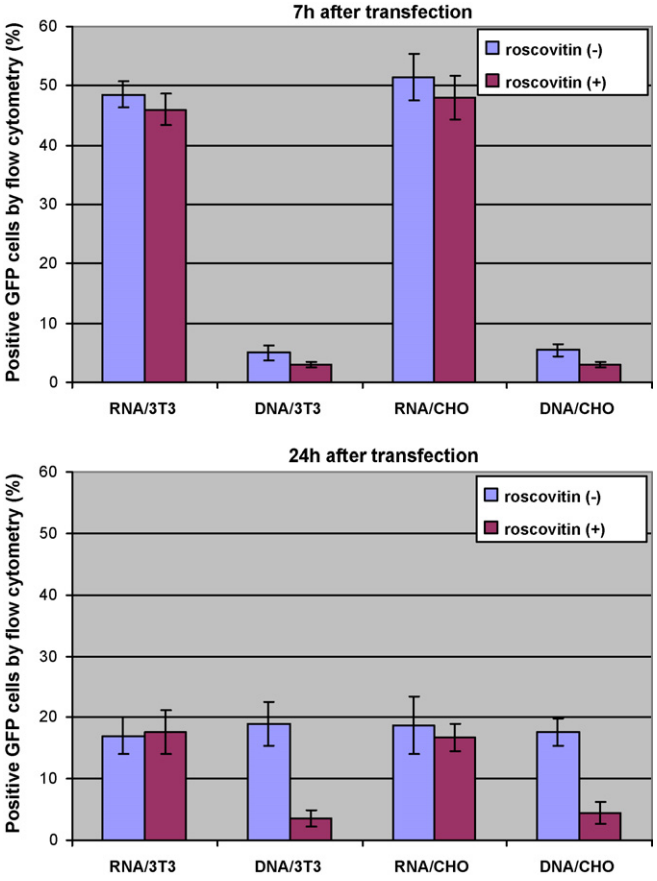

Fig. 5. DNA versus RNA GFP transfections in CHO and NIH3T3 cells with proliferation-inhibition. This figure illustrates the effects of proliferation-inhibition with roscovitine in both CHO and NIH3T3 cells at 7 and 24 h. By 24 h the percent of CHO or NIH3T3 cells positive for GFP is already decreasing after RNA transfection, and is independent of roscovitine treatment. The fraction of cells expressing GFP after GFP DNA transfection in the absence of roscovitine is still increasing at 24 h, but is blocked at a low level by roscovitine.

from 15 to 17% to 4 to 6% in CHO and NIH3T3 cells, respectively. The mean level of expression per cell, as measured by Cell Quest analysis of GFP intensity, was greater than 4 times higher in DNA transfected cells relative to RNA transfected cells.

Figs. 4 and 5 summarize the results of multiple transfections of GFP DNA versus RNA vectors over time. The percent of GFP positive cells by flow cytometry was plotted versus time in hours. Results in the top panel of Fig. 4 show the peak in RNA transfected CHO cells at approximately 7 h, with over 50% transfection, in cells not treated with roscovitine (−). A similar peak after RNA transfection is seen in proliferation-inhibited cells roscovitine (+), also with approximately 50% transfected. The application of roscovitine has no effect on the peak in fraction of cells expressing GFP after transfection with RNA vectors in Fig. 4. This is in contrast to the effect of roscovitine with DNA transfections of CHO cells seen in Fig. 4. The fraction of cells expressing GFP after GFP DNA transfection in the absence of roscovitine (−) is still increasing at 24 h, but is blocked at a low level by roscovitine (+), bottom panel. Roscovitine has no effect on GFP RNA transfections, and the peak at 7 h using RNA vectors in both the presence and absence of roscovitine is clearly illustrated in Fig. 4. DNA transfections, in contrast, were much lower, reaching only 18% in the absence of roscovitine (−), and less than 5% with proliferation-inhibition roscovitine (+).

Fig. 5 illustrates the effects of roscovitine in both CHO and NIH3T3 cells at 7 and 24 h after RNA and DNA transfections, respectively, the time points at which the maximum percentage of cells express GFP. Representative results show the percentage of GFP-expressing cells after RNA transfection at 7 h in roscovitine treated (+) and untreated (−) CHO and NIH3T3 cells. At 7 h RNA transfects approximately 50% of CHO and NIH3T3 cells, independent of roscovitine, but less than 5% of CHO or NIH3T3 cells were transfected by DNA at 7 h either with or without treatment by roscovitine. In contrast, at 24 h, by which time DNA is near peak for the fraction of cells that express GFP, approximately 18% of both CHO and NIH3T3 cells are transfected in the absence of roscovitine, but less than 5% were transfected in the presence of roscovitine. By 24 h the percent of CHO or NIH3T3 cells positive for GFP after RNA transfection is already decreasing, and is independent of roscovitine treatment. The fraction of cells expressing GFP after GFP DNA transfection in the absence of roscovitine is still increasing at 24 h, but is blocked at a low level by roscovitine.

3.1.2. GFP RNA and DNA vector delivery in primary mixed neuronal cells

Next, previously optimized formulations of GFP-encoding RNA and DNA vectors were delivered to primary neurons in culture and were analyzed at 7 and 24 h, the time points of maximum percentage of cells expressing GFP respectively, by flow cytometry. As shown by flow cytometry results in Fig. 6, by 7 h GFP RNA vectors

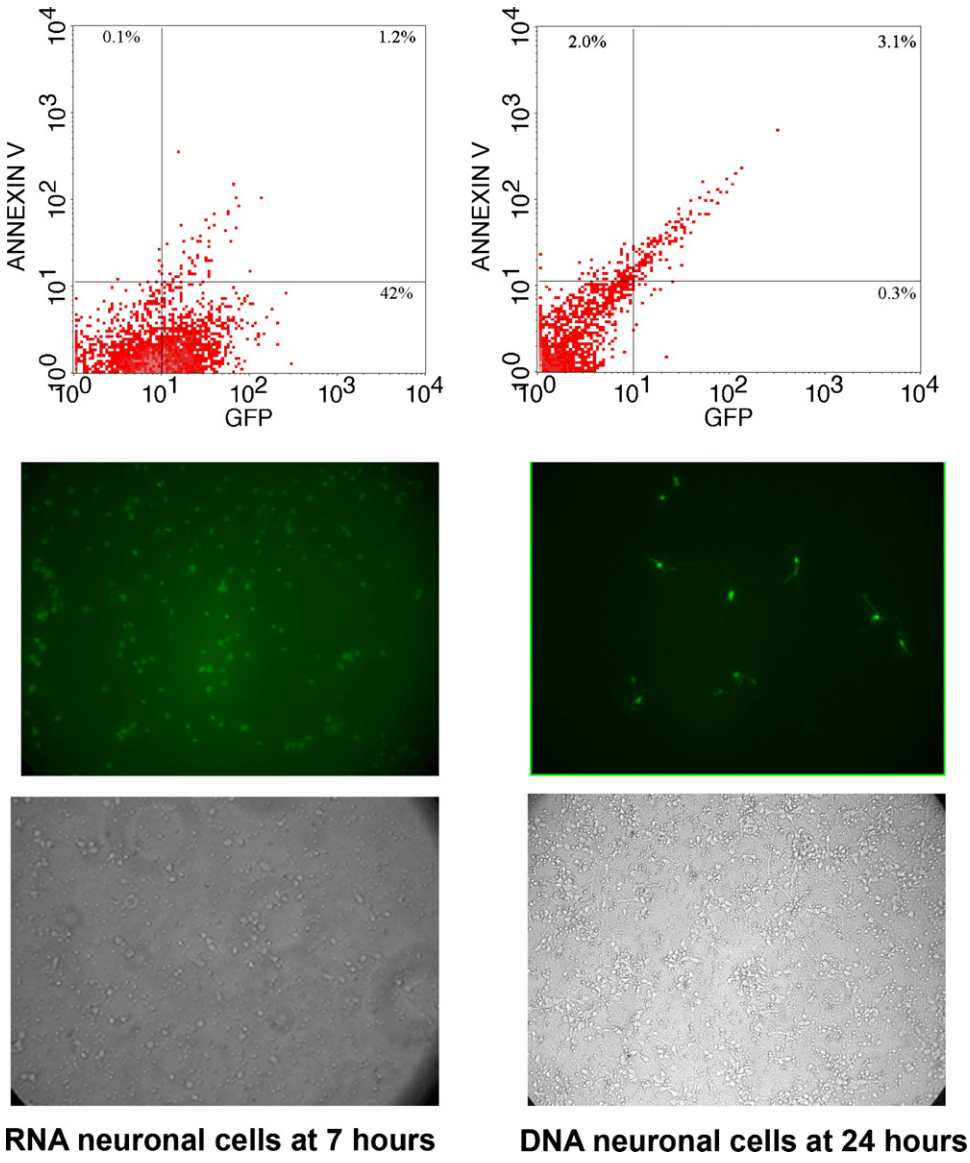

Fig. 6. FACScan analysis of cationic lipid-mediated RNA and DNA transfection in primary mixed neuronal cells. Representative results show the percentage of GFP-expressing cells 7 h and 24 h post-transfection, the time point of maximum percentage of cells expressing GFP, for RNA and DNA, respectively. Flow cytometry results (top panels) show that by 7 h GFP RNA vectors transfected approximately 42% of primary neurons but only 0.3% GFP positive/Annexin negative (lower right quadrant) and 3.1% GFP positive/Annexin positive (upper right quadrant) after transfection with the GFP DNA vector in simultaneous transfections (top right panel).

transfected approximately 42% of primary neurons (top left panel). This compares to approximately 0.3% GFP positive/Annexin negative (lower right quadrant) and 3.1% GFP positive/Annexin positive (upper right quadrant) after transfection with the GFP DNA vector in simultaneous transfections, top right panel in Fig. 6. The corresponding fluorescent and Brightfield digital photographs are shown below each flow cytometry panel. The mean level of expression per cell, as measured by Cell Quest analysis of GFP intensity, was approximately 6 times higher in DNA transfected cells relative to RNA transfected cells. We have achieved results as high as 60% of primary neuronal cells transfected with RNA and 15% with DNA in similar experiments.

3.1.3. Time course of luciferase gene expression after delivery of DNA and RNA to primary neuronal cells

Next, luciferase-encoding DNA and mRNA vectors that had previously been optimized for cationic lipid-mediated formulation were delivered to primary cortical neurons and analyzed every hour for the first 12 h and subsequently at 24, 36, 72, 80, and 96 h. We used luciferase vectors and a cell lysis measurement of luciferase expression rather than GFP and flow cytometry due to the difficulties of producing adequate numbers of identical neuronal cells for simultaneous transfection, and due to the problems associated with analyzing neurons using flow cytometry. The delivery of mRNA to primary cortical neuronal cells resulted in a rapid onset of luciferase expression within 1 h after transfection. Expression peaked at 5–6 h post-transfection, and returned to base line by 12 h after transfection (Fig. 7). DNA delivery resulted in a much later onset of gene expression, beginning approximately 3 h after transfection. DNA gene expression peaked at 36–48 h after transfection, and peak luciferase expression after DNA delivery was generally at least one order of magnitude higher than after RNA deliveryDNA RNA, consistent with our results with GFP vectors as well.

3.1.4. In vivo expression after luciferase-expressing mRNA vector delivery to lateral ventricle

Fig. 8 demonstrates the widespread distribution, uptake and expression that we have achieved after non-viral, cationic lipid-

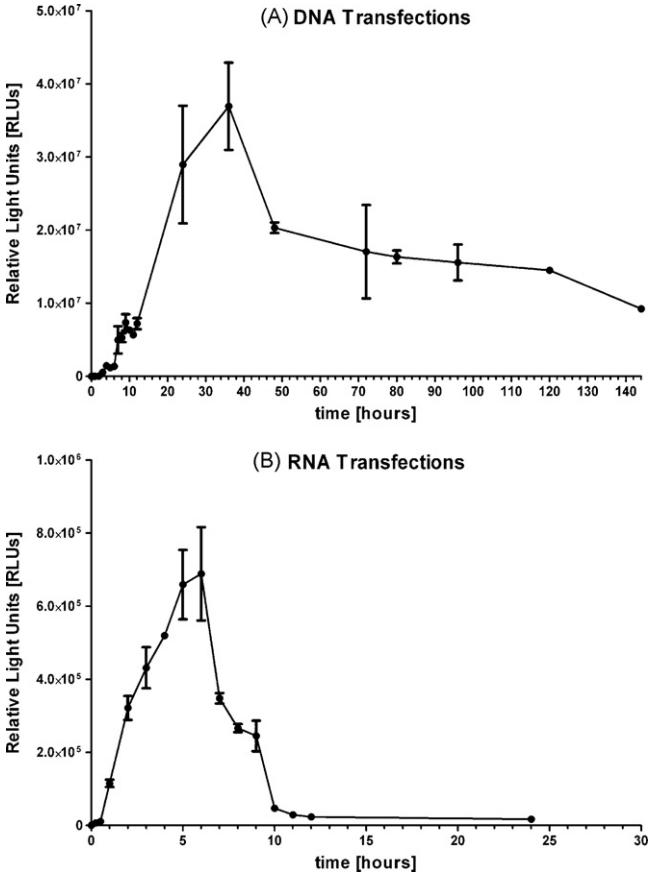

Fig. 7. Time course after RNA and DNA transfection in primary neuronal cells. Luciferase-encoding DNA and mRNA vectors were delivered to primary cortical neurons and analyzed. Delivery of mRNA resulted in a rapid onset of luciferase expression, a peak at 5–6 h post-transfection, and return to base line by 12 h after transfection. DNA gene expression peaked 36–48 h after transfection, Averaged results of three wells at each time point for each experiment, with error bars, are given.

mediated gene delivery of mRNA vectors. In an IACUC approved protocol, we infused optimized formulations of luciferase-encoding mRNA transcripts into the lateral ventricle or cisterna magna of rat brain. Fig. 8A and B demonstrates widespread subcortical expression at 40× magnification from two different animal experiments, in which cells that are phenotypically neurons are clearly visible. Longer DAB staining was used in Fig. 8A. Counterstaining was used in Fig. 8B–H. Fig. 8C is from another animal, at 20× magnification, and shows similar, widespread subcortical expression. Fig. 8D is from an area of Fig. 8C at higher magnification. Fig. 8E is another series from the same animal, and Fig. 8F is from an area of the same section at a 40× magnification. Fig. 8G and H are negative control sections at 20 and 40× respectively, in which the primary antibody has been omitted during immunohistochemistry. 50 μm calibration bars are shown in each panel.

4. Discussion

Gene delivery to, and expression in, non-mitotic cells is essential to the development of gene therapy strategies in the CNS. Although viral methods have been used for some indications, safety issues do not make the routine use of viral transfection optimal or appropriate for many clinical applications (Byk and Scherman, 2000). Cationic lipids are an alternative to viral based gene therapy. Currently, 25% of all clinical trials involve non-viral methods, including 17% using naked/plasmid DNA and 8.3% utilizing cationic lipid-mediated delivery (NOA, 2008).

Systemic infusion to blood plasma has proven to be a difficult medium for gene delivery, because transfection complexes aggregate extensively with polyanionic molecules (Plank et al., 1996; Tros de Ilarduya and Duzgunes, 2000) and are rapidly cleared from the circulation. Degradation and/or aggregation of nucleic acids in the extracellular environment, cellular targeting and uptake of the lipoplex, and release of the nucleic acid sequence from the lipoplex are all major barriers to lipid-mediated transfection. Non-viral lipid-mediated gene transfer to the CNS by cerebrospinal fluid (CSF) delivery avoids many of the difficulties associated with intravascular delivery (Kariko et al., 2001; Hecker et al., 2001). DNA translocation to the nucleus is an additional barrier in the development of an efficient DNA delivery system (Zabner et al., 1995; Bally et al., 1999; Girao da Cruz et al., 2001). In proliferating cells, the majority of the DNA enters the nucleus through passive movement. This occurs during the nuclear membrane degradation stage of mitosis (Wilson et al., 1995; Melchior and Gerace, 1998). However, the amount of DNA that is able to cross the nuclear envelope in non-proliferating cells by passive movement through the NPC has been assumed to be negligible (Aronsohn and Hughes, 1998). Our results indicate that a small percentage of primary neurons can still be transfected with DNA using lipid-mediated delivery techniques, and it is unclear whether this occurs by facilitated uptake by the NPC, simple diffusion, of perhaps by lipid-associated directed trafficking.

We transfected proliferation-inhibited CHO and NIH3T3 cells with either RNA or DNA vectors expressing GFP by using cationic lipid-mediated delivery. Using flow cytometry analysis, we assessed transfection efficiency as a measure of the percentage of cells expressing GFP. 24 h after DNA transfection may not be the peak of luciferase protein expression and accumulation, as the time course for luciferase expression seemed to peak at approximately 36–48 h. Our luciferase assay requires cell lysis and is a measure of total luciferase protein. Signal from the action of luciferase on luciferin will depend on the concentration and activity of the enzyme present. The half-life of GFP in mammalian cells has been reported to be as long as 26 h (Corish and Tyler-Smith, 1999). The half-life of luciferase in mammalian cells is reported to be from 90 min to 4 h (Ignowski and Schaffer, 2004; Allen et al., 2006; University of Arizona, 2008). Two reviews of the kinetics and modeling of luciferase concentration and activity can be found in (Bartlett and Davis, 2006) and (Ignowski and Schaffer, 2004). However we were most interested in the fraction of cells that were transfected rather than the peak in protein expression, which would include intracellular accumulation, and we thus chose to compare flow cytometry results 24 h after DNA delivery and 7 h after RNA delivery based on the peaks in percentage of cells expressing GFP by flow cytometry measurement. We have confirmed these peaks in expression with *in vivo* imaging of both DNA (Hauck et al., 2008) and RNA (data not published) luciferase vectors after CNS delivery.

Transfection efficiency of RNA was greater than that of DNA in proliferation-inhibited CHO and NIH3T3 cells. Our results support the hypothesis that the use of RNA avoids the necessity for nuclear translocation and leads to marked improvements in transfection efficiency over DNA transfection in non-dividing cells. This is similar to Brisson et al. (1999), who used 293 cells expressing T7 bacterial polymerase to show that T7 promoter driven DNA vectors, for which cytoplasmic transcription occurs, provided improved transfection efficiency relative to CMV promoter driven DNA vectors, which require nuclear translocation for transcription (Chapman et al., 1991). However, the T7 system is not applicable to clinical applications. By quantitating the importance of mitosis in DNA transfections and demonstrating the efficiency of mRNA, we

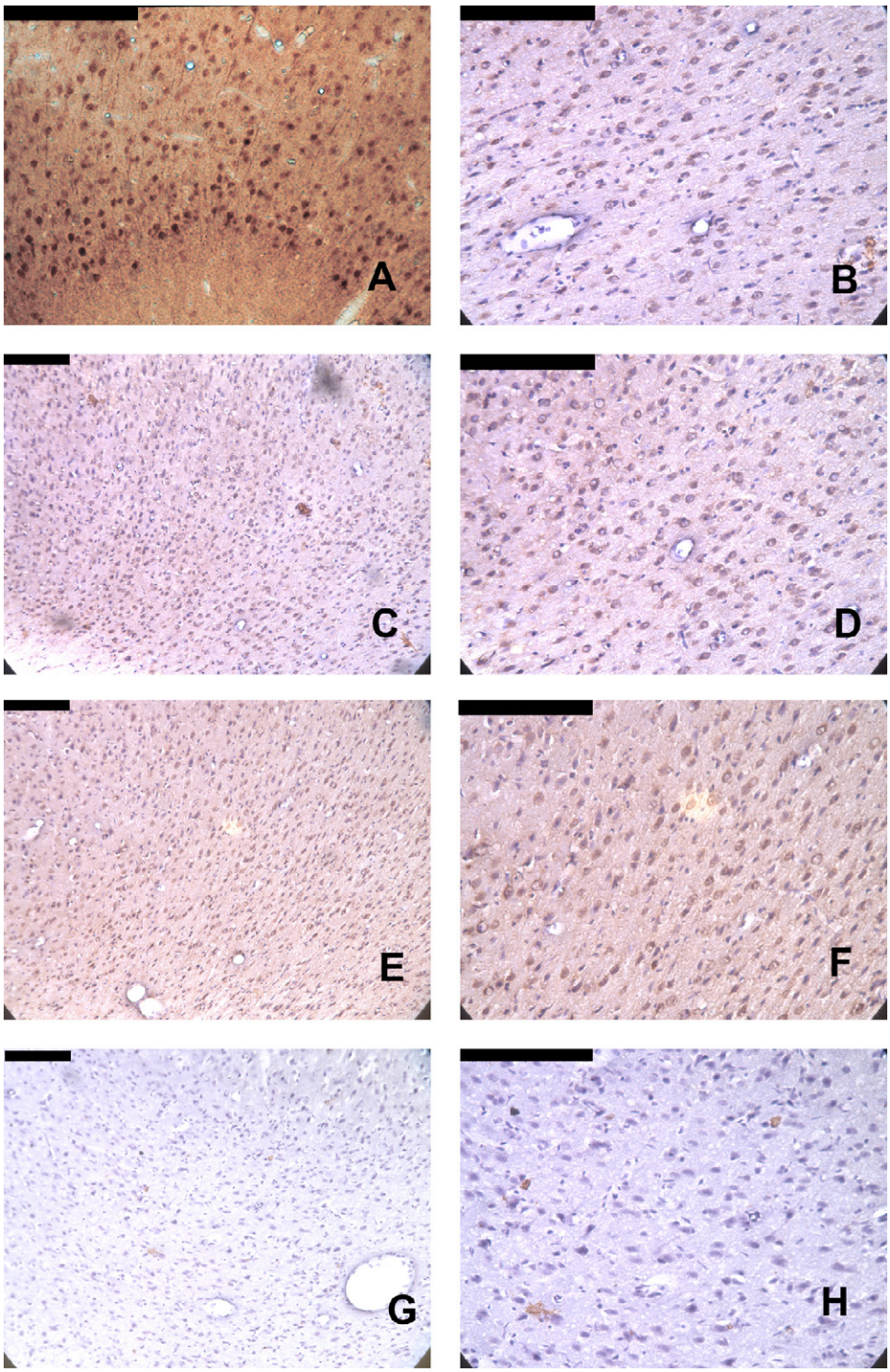

Fig. 8. Representative examples luciferase immunohistochemistry after lipid-mediated RNA lipoplex gene delivery to rat brain via CSF injection. This figure demonstrates the widespread distribution, uptake and expression that we have achieved after non-viral, cationic lipid-mediated gene delivery of mRNA vectors. Subparts A and B demonstrate widespread subcortical expression at 40× magnification from two different animal experiments, with and without counterstaining, in which cells that are phenotypically neurons are clearly visible. Subpart C is an example from another animal, at 20× magnification, and shows similar, widespread subcortical expression. Subpart D is from an area of subpart C at higher magnification. Subpart E is another series from the same animal and subpart F is from an area of the same section at a 40× magnification. Subparts G and H are control sections at 20× and 40× respectively.

confirm that mRNA is a more efficient method for gene delivery to post-mitotic cells.

We repeated these experiments on primary mixed neuronal cultures and observed RNA vector expression levels approaching 50–60%. Higher RNA and DNA transfections in some experiments may be due to variations in glial cell population in these mixed, neuron-enhanced cell populations. Lipid-mediated gene transfer of DNA vectors into primary neurons showed a significantly lower efficiency, transfecting less than 15% of primary neurons, sometimes less than 5%. Maximum expression following RNA vector

delivery was approximately 7 h post-incubation, approximately 24 h earlier than maximum fractional expression levels using DNA vectors. However, the maximum mean level of intensity of GFP expression per cell following RNA delivery was significantly less than that achieved by DNA delivery. Even stabilized RNA transcript vectors are degraded once released from the lipid complex into the cytoplasm. But once DNA crosses the nuclear membrane, multiple mRNA templates can be transcribed, resulting in higher mean levels of expression per cell.

This study allowed us to test fundamental mechanisms of lipid-mediated uptake and cellular expression. This study is novel in that it directly tests the importance of mitosis in the efficiency of lipid-mediated delivery of RNA compared to DNA vectors in proliferation-inhibited CHO cells, proliferation-inhibited NIH3T3 fibroblasts, and in primary neuronal cultures. Our results highlight the importance of mitosis on lipid-mediated transfection efficiency of RNA vs. DNA in proliferation inhibited cell lines and primary neuronal cultures. One goal of all gene delivery should be to match the duration and level of therapeutic gene expression to the specific clinical application, and RNA delivery may be more suited to those clinical applications in which rapid short-term gene expression or gene transfer to post-mitotic cells is required. RNA delivery provides rapid expression, avoids the requirement for DNA nuclear translocation, and achieves high levels of transfection in post-mitotic cells as well. We propose that numerous clinical applications exist for transient gene expression using RNA, or a combination of RNA and DNA gene delivery. Examples include prophylactic delivery of neuroprotective genes to the CNS for prevention of injury during surgical procedures with high risk for CNS ischemia, such as cardiac bypass procedures, thoracic aneurysm repairs, circulation arrested surgical procedures, or neurosurgical resection. Our long-term goal is to use transient gene delivery to the CNS to induce rapid and controllable gene expression for CNS neuroprotection in these patients. Knowledge of the time course, dose response, and level of expression using lipid-mediated DNA or RNA vectors is critical in the translation of *in vitro* techniques to pre-clinical and clinical applications.

Simultaneous or sequential DNA delivery might be used to protect against subsequent cellular loss due to secondary events, including reperfusion injury. RNA can be delivered immediately following CNS trauma (stroke, TBI, SCI) to minimize the initial cellular loss. In such cases, the window of opportunity for effective treatment may be narrow (for example after stroke); therefore the design of an efficient method for rapid gene expression after delivery is essential. We have previously reported on cationic lipid formulations that afford RNA protection from degradation in human CSF for 4 to 6 h, whereas non-complexed RNA is immediately degraded (Anderson et al., 2003). Combining mRNA vectors with delivery to the CSF offers rapid expression in the CNS and avoids the problem of vascular barriers and viral vector safety issues. Finally, these same lipid-mediated lipoplex delivery techniques can be used effectively for siRNA delivery. We have verified knockdown of GFP and luciferase expression *in vitro*, using Transfast and MLRI cationic lipids and similar charge ratios (data not shown).

5. Conclusion

Delivery of mRNA resulted in rapid onset (within 1 h) of expression after transfection, a peak in expression 5–7 h after transfection, and a return to baseline within 12 h. After DNA delivery significant activity did not appear until 7 h after transfection, but peak expression was always at least one order of magnitude higher than after RNA delivery. The peak expression after DNA delivery occurred 24–48 h after transfection and remained at a significant level for at least one week before dropping to baseline. Proliferation is important in DNA expression after transfection, providing strong evidence for the importance of mitosis in uptake of DNA across the nuclear membrane. This is consistent with our *in vivo* delivery results. Qualitatively expression of RNA vectors is equally widespread, but appears to be somewhat less intense than after peak DNA transfection and expression. RNA delivery may therefore be more suitable for short-term transient gene expression due to rapid onset, shorter duration of expression and greater efficiency, particularly in non-dividing cells. Higher mean levels of expression per cell obtained following DNA delivery and the longer duration of expression confirm a continuing role for DNA gene delivery in clinical applications that require longer term transient gene expression. Quantitation of levels of expression and how these relate to clinical physiology remain to be determined.

Acknowledgements

Funding from NIH K08 (JGH), AHA Western States (JGH) and NIH R01 (JGH) is gratefully acknowledged. Primary murine mixed neuronal cells were kindly provided by Candace Floyd, Ph.D. and Phil Washbourne, Ph.D. (UC-Davis), and by Ray Roginski, M.D., Ph.D. (Penn). The generous assistance and training in flow cytometry provided by Carol Oxford (UC-Davis), and Joni Moore, Ph.D. (Penn) is gratefully acknowledged. Scott Fujii, M.S., provided assistance with initial flow cytometry experiments, and Leon Hall performed some of the initial non-neuronal cell experiments that were repeated and extended at the University of Pennsylvania.

References

Allen, M.S., Wilgus, J.R., Chewning, C.S., Sayler, G.S., Simpson, M.L., 2006. A destabilized bacterial luciferase for dynamic gene expression studies. Syst. Synth. Biol. 1, 3–9.

Anderson, D.M., Hall, L.L., Ayyalapu, A., Irion, V.R., Nantz, M.H., Hecker, J.G., 2003. Stability of mRNA/cationic lipid lipoplexes in human and rat cerebrospinal fluid: methods and evidence for non-viral mRNA gene delivery to the CNS. Hum. Gene Ther. 14, 191–202.

Aronsohn, A.I., Hughes, J.A., 1998. Nuclear localization signal peptides enhance cationic liposome-mediated gene therapy. J. Drug Target. 5, 163–169.

Balasubramaniam, R.P., Bennett, M.J., Aberle, A.M., Malone, J.G., Nantz, M.H., Malone, R.W., 1996. Structural and functional analysis of cationic transfection lipids: the hydrophobic domain. Gene Ther. 3, 163–172.

Bally, M.B., Harvie, P., Wong, F.M., Kong, S., Wasan, E.K., Reimer, D.L., 1999. Biological barriers to cellular delivery of lipid-based DNA carriers. Adv. Drug Deliv. Rev. 38, 291–315.

Bartlett, D.W., Davis, M.E., 2006. Insights into the kinetics of siRNA-mediated gene silencing from live-cell and live-animal bioluminescent imaging. Nucleic Acids Res. 34, 322–333.

Bennett, M.J., Nantz, M.H., Balasubramaniam, R.P., Gruenert, D.C., Malone, R.W., 1995. Cholesterol enhances cationic liposome-mediated DNA transfection on human respiratory epithelial cells. Biosci. Rep. 15, 47–53.

Bennett, M.J., Aberle, A.M., Balasubramaniam, R.P., Malone, J.G., Nantz, M.H., Malone, R.W., 1996. Considerations for the design of improved cationic amphiphile-based transfection reagents. J. Liposome Res. 6, 545–565.

Brisson, B., Tseng, W.-C., Almonte, C., Watkins, S., Huang, L., 1999. Subcellular trafficking of the cytoplasmic expression system. Hum. Gene Ther. 10, 2601–2613.

Byk, G., Scherman, D., 2000. Genetic chemistry: tools for gene therapy coming from unexpected directions. Drug Dev. Res. 50, 566–572.

Chapman, B.S., Thayer, R.M., Vincent, K.A., Haigwood, N.L., 1991. Effect of intron A from human cytomegalovirus (Towne) immediate-early gene on heterologous expression in mammalian cells. Nucleic Acids Res. 19, 3979–3986.

Corish, P., Tyler-Smith, C., 1999. Attenuation of green fluorescent protein half-life in mammalian cells. Protein Eng. 12, 1035–1040.

Felgner, P.L., Gadek, T.R., Holm, M., Roman, R., Chan, H.W., Wenz, M., Northrop, J.P., Ringold, G.M., Danielsen, M., 1987. Lipofection: a highly efficient, lipid-mediated DNA-transfection procedure. Proc. Natl. Acad. Sci. 84, 7413–7417.

Felgner, J.H., Kumar, R., Sridhar, C.N., Wheeler, C.J., Tsai, Y.J., Border, R., Ramsey, P., Martin, M., Felgner, P.L., 1994. Enhanced gene delivery and mechanism studies with a novel series of cationic lipid formulations. J. Biol. Chem. 269, 2550–2561.

Felgner, P.L., Tsai, Y.J., Sukhu, L., Wheeler, C.J., Manthorpe, M., Marshall, J., Cheng, S.H., 1995. Improved cationic lipid formulations for in vivo gene therapy. Ann. N.Y. Acad. Sci. 772, 1126–1139.

Flotte, T.R., 2007. Gene therapy: the first two decades and the current state-of-the-art. J. Cell Physiol. 213, 301–305.

Fujii, S., Hall, L., Hecker, J.G., 2002. A comparison of mRNA transfection efficacy and cytotoxicity of 4 cationic lipids in 4 mammalian cell lines. Master of Science. Thesis. Sacramento State University.
Gallie, D.R., Walbot, V., 1990. RNA pseudoknot domain of tobacco mosaic virus can functionally substitute for a poly(A) tail in plant and animal cells. Genes Dev. 4, 1149–1157.
Gao, X., Kim, K.S., Liu, D., 2007. Nonviral gene delivery: what we know and what is next. AAPS J. 9, E92–104.
Girao da Cruz, M.T., Simoes, S., Pires, P.P.C., Nir, S., Pedrosa de Lima, M.C., 2001. Kinetic analysis of the initial steps involved in lipoplex-cell interactions: effect of various factors that influence transfection activity. Biochim. Biophys. Acta 1510, 136–151.
Hauck, E.S., Zou, S., Scarfo, K.A., Nantz, M.H., Hecker, J.G., 2008. Whole animal in vivo imaging after transient non-viral lipid-mediated gene transfer to the rat central nervous system. Mol. Ther. 16, 1857–1864.
Hecker, J.G., Hall, L.L., Irion, V.R., 2001. Non-viral gene delivery to the lateral ventricles in rat brain: initial evidence for widespread distribution and expression in the central nervous system. Mol. Ther. 3, 375–384.
Ignowski, J.M., Schaffer, D.V., 2004. Kinetic analysis and modeling of firefly luciferase as a quantitative reporter gene in live mammalian cells. Biotechnol. Bioeng. 86, 827–834.
Kariko, K., Keller, J.M., Harris, V.A., Langer, D.J., Welsh, F.A., 2001. In vivo protein expression from mRNA delivered into adult rat brain. J. Neurosci. Methods 105, 77–86.
Krisky, D.M., Wolfe, D., Goins, W.F., Marconi, P.C., Ramakrishnan, R., Mata, M., Rouse, R.J.D., 1998. Deletion of multiple immediate-early genes from herpes simplex virus reduces cytotoxicity and permits long-term gene expression in neurons. Gene Ther. 5, 1593–1603.
Li, S.D., Huang, L., 2006. Gene therapy progress and prospects: non-viral gene therapy by systemic delivery. Gene Ther. 13, 1313–1319.
Luo, D., Saltzman, W.M., 2000. Synthetic DNA delivery systems. Nat. Biotechnol. 18, 33–37.
Malone, R.W., Felgner, P.L., Verma, I.M., 1989. Cationic liposome-mediated RNA transfection. Proc. Natl. Acad. Sci. 86, 6077–6081.
Mattaj, I.W., Englmeier, L., 1998. Nucleocytoplasmic transport: the soluble phase. Ann. Rev. Biochem. 67, 265–306.
McKinney, J.S., Willoughby, K.A., Liang, S., Ellis, E.F., 1996. Stretch-induced injury of cultured neuronal, glial, and endothelial cells. Stroke 27, 934–940.
Melchior, F., Gerace, L., 1998. Two-way trafficking with Ran. Trends Cell. Biol. 8, 175–179.
Mortimer, I., Tam, P., MacLachlan, I., Graham, R.W., Saravolac, E.G., Joshi, P.B., 1999. Cationic lipid-mediated transfection of cells in culture requires mitotic activity. Gene Ther. 6, 403–411.
Nicolau, C., Sene, C., 1982. Liposome-mediated DNA transfer in eukaryotic cells. Dependence of the transfer efficiency upon the type of liposomes used and the host cell cycle stage. Biochim. Biophys. Acta 721, 185–190.
Niedzinski, E.J., Fujii, S.K., Lizarzaburu, M.E., Hecker, J.G., Nantz, M.H., 2002. A versatile linker for non-toxic polyamine-mediated DNA transfection. Mol. Ther. 6, 279–286.
NOA, 2008. J. Gene Med., http://www.wiley.co.uk/genetherapy/.
Plank, C., Mechtler, D., Szoka, F.C., Wagner, E., 1996. Activation of the complement system by synthetic DNA complexes: a potential barrier for intravenous gene delivery. Hum. Gene Ther. 7, 1437–1446.
Taymans, C.M., Vandenberghe, L.H., Haute, C.V., Thiry, I., Deroose, C.M., Mortelmans, L., Wilson, J.M., Debyser, Z., Baekelandt, V., 2007. Comparative analysis of adeno-associated viral vector serotypes 1, 2, 5, 7, and 8 in mouse brain. Hum. Gene Ther. 18, 195–206.
Tros de Ilarduya, C., Duzgunes, N., 2000. Efficient gene transfer by transferrin lipoplexes in the presence of serum. Biochim. Biophys. Acta 1463, 333–342.
University of Arizona. Southwest Animal Imaging Resource, 2008. University of Arizona. Ref Type: Pamphlet.
Wangerek, L.A., Dahl, H.H., Senden, T.J., Carlin, J.B., Jans, D.A., Dunstan, D.E., Ioannou, P.A., Williamson, R., Forrest, S.M., 2001. Atomic force microscopy imaging of DNA-cationic liposome complexes optimized for gene transfection into neuronal cells. J. Gene Med. 3, 72–81.
Wells, D.R., Tanguay, R.L., Le, H., Gallie, D.R., 1998. HSP101 functions as a specific translational regulatory protein whose activity is regulated by nutrient status. Genes Dev. 12, 3236–3251.
Wilke, M., Fortunati, E., van den Broek, M., Hoogeveen, A.T., Scholte, B.J., 1996. Efficacy of a peptide-based gene delivery system depends on mitotic activity. Gene Ther. 3, 1133–1142.
Wilson, G.L., Dean, B.S., Wang, G., Dean, D.A., 1995. Nuclear import of plasmid DNA in digitonin-permeabilized cells requires both cytoplasmic factors and specific DNA sequences. J. Biol. Chem. 270, 22025–22032.
Wolff, J.A., Malone, R.W., Williams, P., Chong, W., Acsadi, G., Jani, A., Felgner, P.L., 1990. Direct gene transfer into mouse muscle in vivo. Science 247, 1465–1468.
Zabner, J., Fasbender, A.J., Moninger, T., Poellinger, K.A., Welsh, M.J., 1995. Cellular and molecular barriers to gene transfer by a cationic lipid. J. Biol. Chem. 270, 18997–19007.